Synthesis, Characterization, and Mass-Transport Properties of Two Novel Gadolinium(III) Hexafluoroacetylacetonate Polyether Adducts: Promising Precursors for MOCVD of GdF_3 Films

Graziella Malandrino, Ornella Incontro, Francesco Castelli, and Ignazio L. Fragalà*

Dipartimento di Scienze Chimiche, Università di Catania, V.le Andrea Doria 6, 95125 Catania, Italy

Cristiano Benelli

Dipartimento di Chimica, Università di Firenze, Via Maragliano 77, 50144 Firenze, Italy

Received December 4, 1995. Revised Manuscript Received March 5, 1996[⊗]

The monoglyme $\{CH_3OCH_2CH_2OCH_3\}$ and diglyme $\{CH_3O(CH_2CH_2O)_2CH_3\}$ adducts of the gadolinium trishexafluoroacetylacetonate {Gd(hfa)$_3$·monoglyme (**1**) and Gd(hfa)$_3$·diglyme (**2**)} have been synthesized and characterized by elemental analyses, mass spectrometry, and infrared spectroscopy. Single-crystal X-ray diffraction studies of Gd(hfa)$_3$·diglyme provide evidence of a mononuclear structure. The thermal analyses revealed high volatility and good thermal stability with a low residue for both compounds. The adducts **1** and **2** have better mass-transport properties and thermal behaviors than conventional rare-earth MOCVD precursors and have been successfully applied to GdF_3 film depositions. They represent the first examples of gadolinium precursors that can be used in the liquid phase without decomposition, thus providing constant evaporation rates even for very long deposition times.

Introduction

Lanthanide β-diketonates have been widely studied for many years,[1−4] and recently they have also attracted even more attention because of their wide range of applications. Among lanthanide metals, gadolinium represents an interesting element since it plays an important role in a large variety of materials from high-T_c superconductors[5,6] to NMR shift reagents,[1] from thin films of $GdAlO_3$[7] and $GdAl_{11}O_{18}$[7] to scintillator materials[8] and from solid oxide fuel cell to GdF_3 and GdOF host matrixes.[9]

MOCVD (metal−organic chemical vapor deposition)[10] has proven a very powerful technique for most of these applications. In fact, it offers some advantages, such as simplified apparatus, lower deposition temperatures, ability to coat complex shapes, and adaptability to large-scale processing, if compared to classical physical techniques. In addition, it produces films of good quality even for those applications where high performances are required as, for example, the deposition of epitaxial Pr-doped BaF_2 on CaF_2 substrate for optical waveguide applications.[11]

The MOCVD deposition of GdF_3 is hampered by the lack of suitable thermally stable and highly volatile gadolinium precursors. As a matter of fact, the use of the "first generation" $[Gd(tmhd)_3]_2$ (Htmhd = 2,2,6,6-tetramethylheptane-3,5-dione) precursor requires the use of an additional fluorine source similarly to that previously reported for the synthesis of LnF_3 from the $Ln(tmhd)_3·H_2O$ precursors.[12] On the other hand, problems are associated with the simpler "Gd(hfa)$_3$", since its nature is strictly related to the synthetic route used for the preparation[13,14] and, in any case, even the simpler $Gd(hfa)_3·2H_2O$ is not very volatile and gives rise to decomposition.[13b]

This observation prompted investigations on suitable fluorinated and highly chelating molecular architecture of the ligand framework in order (i) to have an internal fluorine source, (ii) to avoid oligomerization, and (iii) to

* To whom correspondence should be addressed.

[⊗] Abstract published in *Advance ACS Abstracts,* April 1, 1996.

(1) Mehrotra, R. C.; Bohra, R.; Gaur, D. P. *Metal β-diketonates and Allied Derivatives*; Academic Press: London, 1978.

(2) Bradley, D. C.; Mehrotra, R. C.; Gaur, D. P. *Metal Alkoxides*; Academic Press: London, 1978.

(3) Sievers, R. E.; Sadlowski, J. E. *Science* **1978**, *201,* 217.

(4) Mehrotra, R. C.; Singh, A.; Tripathi, U. M. *Chem. Rev.* **1991**, *91,* 1287.

(5) Yang, K. N.; Dalichaouch, Y.; Ferreira, J. M.; Lee, B. W.; Neumeier, J. J.; Torikachvili, M. S.; Zhou, H.; Maple, M. B.; Hake, R. R. *Solid State Commun.* **1987**, *63,* 515.

(6) Engler, E. M.; Lee, V. Y.; Nazzal, A. I.; Beyers, R. B.; Lim, G.; Grant, P. M.; Parkin, S. S. P.; Ramirez, M. L.; Vasquez, J. E.; Savoy, R. J. *J. Am. Chem. Soc.* **1987**, *109,* 2848.

(7) Vaidya, K. J.; Yang, C. Y.; DeGraef, M.; Lange, F. F. *J. Mater. Res.* **1994**, *9,* 410.

(8) Blasse, G. *Chem. Mater.* **1994**, *6,* 1465.

(9) (a) Hölsä, J.; Kestilä, E. *J. Chem. Soc., Faraday Trans.* **1995**, *91,* 1503. (b) Hölsä, J.; Kestilä, E. *J. Alloy Comp.* **1995**, *225,* 89.

(10) (a) *Chemical Vapor Deposition: Principles and Applications* (Hitchman, M. L., Jensen, K. F., Eds.; Academic Press: London, 1993. (b) Spencer, J. T. In *Progress in Inorganic Chemistry*; (Karlin, K. D., Ed.; John Wiley & Sons Inc.: New York, 1994; Vol. 41, p 145.

(11) Sato, H. *Jpn. J. Appl. Phys.* **1994**, *33,* L371.

(12) Amano, R.; Shiokawa, Y.; Sato, N.; Suzuki, Y. *J. Radioanal. Nucl. Chem.* **1993**, *172,* 81.

(13) (a) Richardson, M. F.; Wagner, W. F.; Sands, D. E. *J. Inorg. Nucl. Chem.* **1968**, *30,* 1275. (b) Richardson, M. F.; Sievers, R. E. *Inorg. Chem.* **1971**, *10,* 498.

(14) Plakatouras, J. C.; Baxter, I.; Hursthouse, M. B.; Abdul Malik, K. M.; McAleese, J.; Drake, S. R. *J. Chem. Soc., Chem. Commun.* **1994**, *2455.*

S0897-4756(95)00569-2 CCC: $12.00

improve the thermal stability, volatility, and mass-transport properties of the precursor. It is well-known that the combined use of fluorinated β-diketonates and of an ancillary coordinated polyether provides monomeric, volatile and thermally stable alkaline-earth metal precursors.[15−20] The same strategy has been applied to the lanthanide metals and the tailoring of the molecular architecture of the ligands has yielded thermally stable, volatile, and very promising lanthanum MOCVD precursors.[21]

Herein, we report the synthesis, characterization, and mass-transport properties of the water-free single-source precursors Gd(hfa)$_3$·L (Hhfa = hexafluoroacetylacetone, L = dimethoxyethane, *monoglyme*, and bis(2-methoxyethyl)ether, *diglyme*) for MOCVD of GdF_3. Their thermal stabilities and their volatiles compared to conventional gadolinium sources, and preliminary results of their application to MOCVD of GdF_3 are discussed.

Experimental Procedure

Reagents. Gd_2O_3, Hhfa, monoglyme, and diglyme were purchased from Aldrich and used without further purification.

General Procedures. Elemental microanalyses were performed in the Analytical Laboratories of the University of Catania. Infrared data were collected on a 684 Perkin-Elmer spectrometer either as Nujol or hexachlorobutadiene mulls between KBr plates. Thermal measurements were made using a Mettler 3000 system equipped with a TG 50 thermobalance, a TC 10 processor, and DSC 30 calorimeter. The weight of the samples investigated was between 13−15 mg (TG) and 4−6 mg (DSC). Analyses were made under prepurified nitrogen using a 5 °C/min heating rate. The atmospheric pressure volatilization rate TG experiments were carried out with a temperature ramp up of 3 °C/min under N_2 and with a 4 mm sample pan. FAB mass spectra were obtained by using a Kratos MS 50 spectrometer. The melting points were measured in air with a Koffler instrument.

Synthesis of Gd(hfa)$_3$·monoglyme (1). Gd_2O_3 (1.751 g, 4.83 mmol) was first suspended in *n*-hexane (60 mL). Monoglyme (0.849 g, 9.42 mmol) was added to the suspension. Hhfa (5.880 g, 28.26 mmol) was added under vigorous stirring after 10 min, and the mixture was refluxed under stirring for 2 h. The excess of gadolinium oxide was filtered off. On cooling, white crystals separated from the mother liquor. The crystalline white solid was collected by filtration and dried under vacuum. The yield was 91%. The melting point of the crude product was 80−81 °C/760 mmHg. Anal. Calcd for $GdC_{19}H_{13}F_{18}O_8$: C, 26.27; H, 1.51. Found: C, 26.58; H, 1.78. The adduct quantitatively sublimes at 75−80 °C/10^{-3} mmHg. MS (dry FAB; *m*/*z* (fragment), M = Gd(hfa)$_3$·monoglyme):[22] 664 $(M-hfa)^+$ 100%, 476 $(M-2hfa+F)^+$ 52%, 386 $(M-2hfa-monoglyme+F)^+$ 15%, 288 $(M-3hfa+2F)^+$ 41%, 198 $(GdF_2)^+$ 68%. IR (hexachlorobutadiene; ν, cm^{-1}): 2930 (s), 1650 (vs), 1615 (vw), 1565 (m), 1540 (m), 1500 (ms), 1465 (m), 1380 (w), 1350 (vw), 1250 (s), 1210 (s), 1160 (sh), 1100 (m), 1045 (m), 1020 (vw), 950 (vw), 865 (w), 805 (m), 740 (w), 660 (m), 595 (mw).

The MS and IR data of the raw and sublimed adduct are identical. The paramagnetism of the gadolinium(III) ion has precluded solution NMR studies.

Synthesis of Gd(hfa)$_3$·diglyme (2). Prepared as described for the monoglyme adduct from 1.743 g (4.80 mmol) of Gd_2O_3, 5.880 g (28.26 mmol) of Hhfa, and 1.264 g (9.42 mmol) of diglyme. Yield 88%. Melting point: See DSC section. Anal. Calcd for $GdC_{21}H_{17}F_{18}O_9$: C, 27.64; H, 1.88. Found: C, 27.81; H, 1.89. The adduct quantitatively sublimes at 75−85 °C/10^{-3} mmHg. MS (dry FAB; *m*/*z* (fragment), M = Gd(hfa)$_3$·diglyme):[22] 708 $(M-hfa)^+$ 100%, 575 $(M-hfa-diglyme)^+$ 15%, 520 $(M-2hfa+F)^+$ 51%, 386 $(M-2hfa-diglyme+F)^+$ 11%, 332 $(M-3hfa+2F)^+$ 49%, 198 $(GdF_2)^+$ 11%. IR (hexachlorobutadiene or Nujol; ν, cm^{-1}): 2930 (s), 1650 (vs), 1555 (m), 1530 (m), 1495 (s), 1455 (s), 1380 (m), 1350 (w), 1255 (vs), 1200 (vs), 1140 (vs), 1095 (sh), 1070 (m), 1060 (m), 1040 (m), 1010 (w), 975 (m), 945 (w), 865 (m), 830 (w), 800 (sh), 790 (m), 760 (w), 730 (mw), 650 (m), 590 (mw).

The MS and IR data of the raw and sublimed adduct are identical.

Table 1. Crystal Data and Structure Refinement for Gd(hfa)$_3$·diglyme

empirical formula	$GdC_{21}H_{17}F_{18}O_9$
formula weight	912.60
temp	293(2) K
wavelength	0.71069 Å
crystal system	monoclinic
space group	$P2_1/n$
unit-cell dimensions	a = 10.228(2) Å, α = 90.000(10)°
	b = 16.065(2) Å, β = 95.960(10)°
	c = 19.401(3) Å, γ = 90.000(10)°
volume	3170.6(9) Å^3
Z	4
density (calculated)	1.912 Mg/m^3
absorption coefficient	2.242 mm^{-1}
F(000)	1764
crystal size	0.17 × 0.22 × 0.31 mm
θ range for data collection	2.51−26.98°
index ranges	$-13 \le h \le 12$, $0 \le k \le 20$, $0 \le l \le 24$
reflections collected	6976
independent reflections	6780 [R(int) = 0.1801]
refinement method	full-matrix least-squares on F^2
data/restraints/parameters	6775/0/499
goodness-of-fit on F^2	1.016
final R indexes [$I > 2\sigma(I)$]	R_1 = 0.0871, wR_2 = 0.2592
R indexes (all data)	R_1 = 0.1025, wR_2 = 0.2923
largest diff peak and hole	3.206 and −4.050 e Å^{-3}

X-ray Structural Determination of Gd(hfa)$_3$·diglyme. The complex was recrystallized from hexane. A 0.17 × 0.22 × 0.31 mm colorless crystal was mounted at the end of a quartz fiber. X-ray data were collected on an Enraf-Nonius CAD 4 four-circle diffractometer, using Mo Kα radiation (λ = 0.710 69 Å). Unit-cell parameters were derived from least-squares refinements of setting angles of 25 reflections in the $9 < \theta < 15°$ range and are reported in Table 1 with other experimental parameters. Corrections were applied for Lorentz and polarization effects. Attempts to account for absorption by using the DIFABS package did not improve the final refinement. The reflections were, therefore, used without corrections. The reflections were processed by the direct method program SIR 92, which provided a satisfactory set of atomic parameters for gadolinium and oxygen atoms. The other atomic parameters were determined by conventional Fourier difference syntheses and the whole set was refined by using the SHELX93 package up to the final results listed in Table 2. Anisotropic displacement parameters were introduced for all non-hydrogen atoms. The hydrogen atoms were included as idealized atoms riding on the respective carbon atoms with C−H bond lengths appropriate to the carbon atom hybridization. The isotropic displacement parameters of each hydrogen atom was fixed at 1.5 times the equivalent isotropic displacement parameters of the carbon to which is bounded.

Some difficulties were found in the refinement procedure due to the disorder present in the CF_3 groups of the hexafluo-

(15) Timmer, K.; Spee, K. I. M. A.; Mackor, A.; Meinema, H. A.; Spek, A. L.; Van der Sluis, P. *Inorg. Chim. Acta* **1991**, *190*, 109.
(16) Gardiner, R.; Brown, D. W.; Kirlin, P. S.; Rheingold, A. L. *Chem. Mater.* **1991**, *3*, 1053.
(17) Drake, R. S.; Miller, S. A. S.; Williams, D. J. *Inorg. Chem.* **1993**, *32*, 3227.
(18) Neumayer, D. A.; Studebaker, D. B.; Hinds, B. J.; Stern, C. L.; Marks, T. J. *Chem. Mater.* **1994**, *6*, 878.
(19) (a) Malandrino, G.; Fragalà, I. L.; Neumayer, D. A.; Stern, C. L.; Hinds, B. J.; Marks, T. J. *J. Mater. Chem.* **1994**, *4*, 1061. (b) Shamlian, S. H.; Hitchman, H. L.; Cook, S. L.; Richards, B. C. *J. Mater. Chem.* **1994**, *4*, 81.
(20) Malandrino, G.; Castelli, F.; Fragalà, I. L. *Inorg. Chim. Acta* **1994**, *224*, 203.
(21) Malandrino, G.; Licata, R.; Castelli, F.; Fragalà, I. L.; Benelli, C. *Inorg. Chem.* **1995**, *34*, 6233.
(22) The given *m*/*z* ratios are related to the isotope ^{160}Gd.

Table 2. Atomic Coordinates ($\times 10^4$) and Equivalent Isotropic Displacement Parameters ($A^2 \times 10^3$) for $Gd(hfa)_3 \cdot diglyme$[a]

	x	*y*	*z*	*U*(eq)[a]
Gd(1)	7572(1)	1040(1)	7624(1)	49(1)
O(1)	6359(7)	1806(4)	6704(3)	64(2)
O(2)	5491(6)	405(5)	7434(4)	67(2)
C(11)	5264(11)	1678(6)	6362(5)	64(2)
C(12)	4368(12)	1076(7)	6479(8)	70(3)
C(13)	4498(10)	516(7)	7010(6)	67(2)
C(14)	4946(14)	2257(9)	5756(7)	89(4)
F(111)	4351(25)	2003(28)	5261(21)	126(12)
F(112)	3794(20)	2116(19)	5373(16)	92(7)
F(121)	5950(34)	2619(26)	5530(18)	138(13)
F(122)	5750(46)	1979(24)	5226(14)	179(16)
F(131)	5294(65)	2985(17)	5828(19)	181(32)
F(132)	4296(35)	2927(18)	6019(18)	139(12)
C(15)	3413(14)	−76(12)	7108(9)	103(5)
F(14)	2278(8)	125(9)	6817(8)	163(6)
F(15)	3277(19)	−213(17)	7742(10)	233(11)
F(16)	3601(18)	−787(8)	6883(18)	280(17)
O(3)	6011(7)	1944(5)	8100(4)	65(2)
O(4)	7425(6)	675(5)	8812(3)	59(2)
C(21)	5446(9)	1935(6)	8636(5)	59(2)
C(22)	5730(12)	1443(8)	9228(6)	71(3)
C(23)	6737(13)	896(7)	9259(6)	68(3)
C(24)	4256(15)	2524(9)	8618(9)	85(4)
F(211)	4717(44)	3299(27)	8800(33)	193(26)
F(212)	4496(45)	3228(18)	8385(29)	146(18)
F(221)	3349(20)	2258(26)	8127(24)	151(16)
F(222)	3784(31)	2706(30)	8028(20)	139(11)
F(231)	3780(62)	2585(45)	9226(26)	185(31)
F(232)	3462(48)	2384(36)	9003(27)	152(19)
C(25)	7130(14)	436(9)	9970(7)	82(3)
F(24)	6967(23)	−334(8)	9917(6)	187(8)
F(25)	8393(15)	445(14)	10127(7)	206(9)
F(26)	6662(27)	719(12)	10476(6)	262(13)
O(5)	9109(7)	1742(5)	6987(4)	64(2)
O(6)	7764(8)	309(4)	6550(4)	72(2)
C(31)	9449(10)	1687(7)	6382(6)	65(2)
C(32)	9045(17)	1117(8)	5872(7)	80(4)
C(33)	8178(12)	486(7)	6000(6)	68(2)
C(34)	10433(16)	2342(9)	6206(8)	89(4)
F(31)	11119(12)	2152(7)	5701(7)	142(5)
F(32)	9784(18)	3009(7)	5980(13)	224(12)
F(33)	11225(22)	2554(15)	6722(9)	244(13)
C(35)	7813(18)	−117(12)	5404(8)	98(4)
F(36)	6567(14)	−220(12)	5323(8)	186(7)
F(37)	8181(18)	−861(9)	5524(10)	176(7)
F(38)	8237(18)	39(12)	4826(6)	186(7)
C(41)	7219(16)	−1011(7)	8251(10)	89(4)
O(7)	7900(8)	−510(4)	7790(4)	71(2)
C(42)	9269(14)	−722(8)	7766(7)	82(3)
C(43)	10054(11)	−266(8)	8296(7)	82(3)
O(8)	9836(6)	607(5)	8147(4)	68(2)
C(44)	10530(14)	1115(9)	8679(9)	83(4)
C(45)	10259(12)	1996(9)	8483(8)	87(4)
O(9)	8873(7)	2146(5)	8373(4)	70(2)
C(46)	8645(16)	2984(9)	8384(11)	109(5)

[a] For the atom numbering see Figure 3. [b] *U*(eq) is defined as one third of the trace of the orthogonalized U_{ij} tensor.

roacetylacetonate moieties. Several attempts were made to find a model for these disordered groups. The best results were obtained when considering for two of them, two different sets of fluorine atoms with a fractional site occupation factors fixed at 0.5 each. No improvement was observed by considering rigid CF_3 groups. In the final stage of refinement a peak of intensity of 3.04 e $Å^{-3}$ was observed on the Fourier difference map. The peak is located at about 1.5 Å from two fluorine atoms of a CF_3 group. Any attempt to attribute this peak to an atom failed, so it was not assigned.

MOCVD Experiments. Low-pressure MOCVD depositions were performed using a horizontal hot-wall reactor from $Gd(hfa)_3 \cdot$monoglyme or $Gd(hfa)_3 \cdot$diglyme precursors contained in a resistively heated alumina boat at 110 °C. The volatile precursor was transported to the resistively heated zone by O_2 as a carrier gas at 50 cm^3/min (STP). The glass and (111) Si substrates were degreased by sonication in methanol for 20 min. The substrate temperature was varied in the range 400−600 °C, the run time was 1 h, and the total pressure 3 Torr.

X-ray diffraction $\theta/2\theta$ scans were recorded on a computer interfaced Philips diffractometer using Ni-filtered Cu Kα radiation at 20 mA/40 kV.

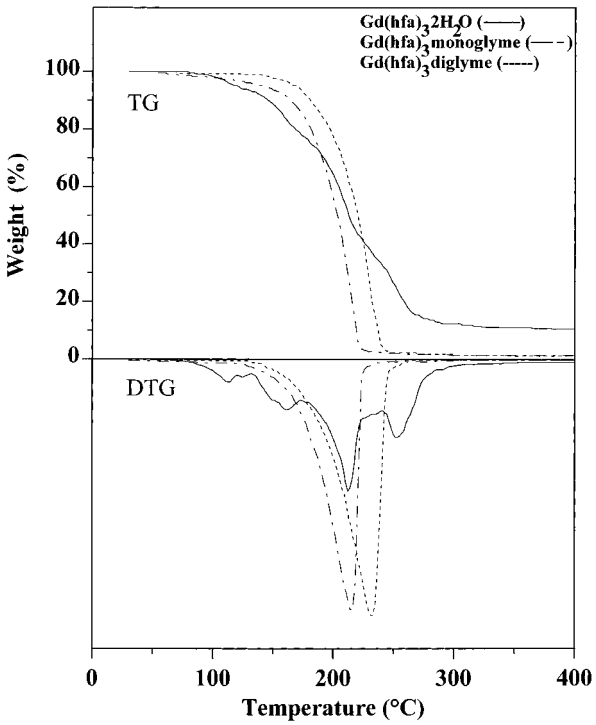

Figure 1. TG-DTG curves of the $Gd(hfa)_3 \cdot$monoglyme and $Gd(hfa)_3 \cdot$diglyme adducts compared to the parent $Gd(hfa)_3 \cdot 2H_2O$.

Results

Synthesis. The single-step reaction of the gadolinium oxide with hexafluoroacetylacetone and polyether in *n*-hexane (eq 1) has been found to yield reproducibly

$$^1/_2Gd_2O_3 + 3Hhfa + 1\ \text{polyether} \rightarrow Gd(hfa)_3 \cdot \text{polyether} \quad (1)$$

anhydrous, air-stable adducts in air. The adducts are soluble in common organic solvents such as ethanol, chloroform, acetone, pentane, benzene, toluene, and slightly soluble in cyclohexane. The adducts **1** and **2** sublime at 75−80 and 75−85 °C (10^{-3} mmHg), respectively. They are nonhygroscopic and can be handled in air.

Thermogravimetric and Calorimetric Data. The thermal behavior of the raw adducts **1** and **2** has been studied by thermal gravimetric analysis (TG), differential thermal gravimetric analysis (DTG) and differential scanning calorimetry (DSC) under N_2 as carrier gas. The TG curves of **1** and **2** show singular sublimation steps (Figure 1) in the 110−268 °C (residue = 3% to 280 °C) and 105−296 °C (residue = 4% to 280 °C) temperature ranges, respectively. 50% weight losses are observed (under the present operating conditions) at 206 and 220 °C for **1** and **2**, respectively. The TG curve of the $Gd(hfa)_3 \cdot 2H_2O$[23] parent complex (Figure 1) shows more steps in the 75−325 °C (residue = 13% to

(23) The $Gd(hfa)_3 \cdot 2H_2O$ has been synthesized as reported in ref 13.

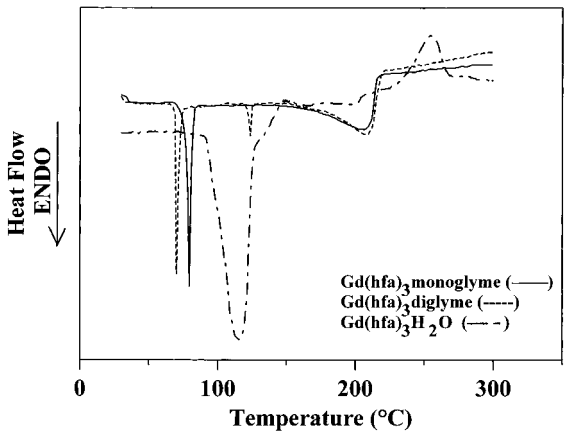

Figure 2. DSC curves of the $Gd(hfa)_3 \cdot 2H_2O$ and the $Gd(hfa)_3 \cdot$ monoglyme and $Gd(hfa)_3 \cdot$diglyme adducts.

380 °C) temperature range, due to the decomposition of the chelate to nonstoichiometric products, probably through reactions of the type $LnL_3(H_2O) \rightarrow LnL_2OH + HL$.[13b]

The DSC curves of $Gd(hfa)_3 \cdot L$ adducts and of the parent $Gd(hfa)_3 \cdot 2H_2O$ are reported in Figure 2. The sharp melting point at 80.7 °C (−9.23 cal/g) observed for **1** closely agrees with the actual melting point. Sublimation from the melt occurs afterward. The DSC curve of the diglyme adduct **2** shows some interesting features. Two sharp endothermic peaks are observed at 69.8 °C (−9.07 cal/g) and 123.3 °C (−0.95 cal/g). Several consecutive heating and cooling DSC experiments in the 30−150 °C temperature range have shown the disappearance of the first peak after the first cycle. The second peak, by contrast, remains unchanged as far as both the temperature and the ΔH associated with the process are concerned. The peak at 69.8 °C becomes again evident after several hours standing at room temperature. This endothermic process is likely associated with a transition from the solid to a plastic phase.[24] This conclusion agrees well with the visual observation of the sample around 90 °C as well as with optical microscopy observations during the heating cycle. The second peak is associated with the complete clarification. Note, in this context, that this property implies that the sample can be used in the 90−100 °C temperature range under MOCVD conditions in the plastic phase, thus avoiding all the problems associated with grain dimensions. The DSC curve of $Gd(hfa)_3 \cdot 2H_2O$ (Figure 2) shows two endothermic and one exothermic peaks. The endothermic peak at 115.9 °C (−42.94 cal/g) is associated with the melting, while the very broad endothermic peak between 140 and 250 °C is associated with a partial sublimation of the product. The exothermic peak at 260 °C is likely related to a decomposition process involving the loss of HL as reported in earlier studies.[13b] Note that the TG weight loss (22.9%) associated with this exothermic peak agrees well with the calculated value (25.4%) for the loss of an HL ligand.

Finally, note that the MS, IR spectra, and thermal properties of the present raw materials remain identical after several sublimation cycles in vacuo.

Mass Spectra. The FAB spectra of adducts **1** and **2** show peaks due to the loss of both the Hhfa ligand and the polyether. Peaks arising from the characteristic fluorine-transfer process, already observed in the spectra of the alkaline-earth β-diketonate polyether adducts[19a] have been observed. The presently observed MS peaks are associated with $[Gd(hfa)_2 \cdot \text{polyether}]^+$, $[Gd(hfa) \cdot \text{polyether}+F]^+$, $[Gd(hfa)_2]^+$, $[Gd(hfa)+F]^+$, $[Gd \cdot \text{polyether}+2F]^+$, and $[GdF_2]^+$ fragments. No molecular ion peaks or peaks at higher mass have been observed according to the monomeric nature of the complexes.

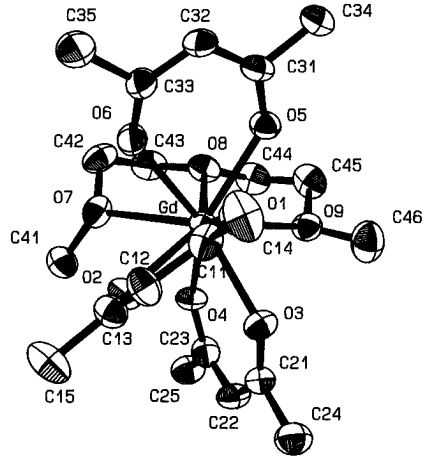

Figure 3. ORTEP drawings of the crystal structure of $Gd(hfa)_3 \cdot$diglyme. CF_3 groups have been omitted for clarity.

Table 3. Selected Bond Lengths (Å) and Angles (deg) for $Gd(hfa)_3 \cdot$diglyme

		Bond	
Gd(1)−O(2)	2.354(7)	Gd(1)−O(5)	2.381(7)
Gd(1)−O(4)	2.399(6)	Gd(1)−O(1)	2.403(7)
Gd(1)−O(3)	2.412(7)	Gd(1)−O(6)	2.417(7)
Gd(1)−O(8)	2.527(7)	Gd(1)−O(7)	2.528(7)
Gd(1)−O(9)	2.578(8)		
		Angles	
O(2)−Gd(1)−O(5)	139.4(3)	O(2)−Gd(1)−O(4)	84.2(2)
O(5)−Gd(1)−O(4)	136.4(2)	O(2)−Gd(1)−O(1)	73.6(2)
O(5)−Gd(1)−O(1)	72.0(3)	O(4)−Gd(1)−O(1)	139.4(2)
O(2)−Gd(1)−O(3)	72.4(3)	O(5)−Gd(1)−O(3)	114.3(3)
O(4)−Gd(1)−O(3)	70.7(2)	O(1)−Gd(1)−O(3)	70.4(2)
O(2)−Gd(1)−O(6)	79.0(3)	O(5)−Gd(1)−O(6)	70.5(2)
O(4)−Gd(1)−O(6)	136.8(2)	O(1)−Gd(1)−O(6)	72.0(3)
O(3)−Gd(1)−O(6)	137.6(3)	O(2)−Gd(1)−O(8)	136.0(3)
O(5)−Gd(1)−O(8)	73.3(2)	O(4)−Gd(1)−O(8)	72.1(2)
O(1)−Gd(1)−O(8)	145.1(2)	O(3)−Gd(1)−O(8)	128.8(3)
O(6)−Gd(1)−O(8)	93.4(3)	O(2)−Gd(1)−O(7)	72.5(3)
O(5)−Gd(1)−O(7)	116.5(3)	O(4)−Gd(1)−O(7)	70.0(2)
O(1)−Gd(1)−O(7)	130.6(3)	O(3)−Gd(1)−O(7)	129.0(2)
O(6)−Gd(1)−O(7)	67.0(2)	O(8)−Gd(1)−O(7)	64.8(3)
O(2)−Gd(1)−O(9)	142.4(3)	O(5)−Gd(1)−O(9)	68.6(3)
O(4)−Gd(1)−O(9)	72.9(3)	O(1)−Gd(1)−O(9)	105.2(3)
O(3)−Gd(1)−O(9)	72.1(3)	O(6)−Gd(1)−O(9)	137.5(3)
O(8)−Gd(1)−O(9)	64.2(3)	O(7)−Gd(1)−O(9)	123.6(3)

Infrared Spectra. The IR spectra of the raw and sublimed $Gd(hfa)_3 \cdot$polyether adducts are identical. The absence of any structure in the 3300−3600 cm^{-1} interval is indicative of no water coordinated to the gadolinium ion. Note that, a broad band at 3500 cm^{-1} is a clear indication of water coordination in the $Gd(hfa)_3 \cdot 2H_2O$ spectrum.[13]

X-ray Crystal Structure of $Gd(hfa)_3 \cdot$diglyme. The ORTEP drawing of the asymmetric unit of the $Gd(hfa)_3 \cdot$diglyme is shown in Figure 3. Positional parameters and selected bond distances and angles are reported in Tables 2 and 3, respectively. The crystal structure of **2** consists of a mononuclear complex with the gadolinium ion in a nine-coordination sphere formed

(24) Malandrino, G.; Fragalà, I. L., unpublished results.

by the six oxygen atoms of the three hfa ligands and by the three oxygen atoms of the diglyme ligand. The Gd−O distances associated with the hfa ligands (Gd−O_{hfa}) lie in the range 2.354(7)−2.417(7) Å (average 2.394 Å), while those associated with the diglyme (Gd−$O_{diglyme}$) lie in the range 2.527(7)−2.578(8) Å (average 2.544 Å). The presently observed Gd−O_{hfa} distances are slightly longer than those reported for eight-coordinated compounds containing the Gd(hfa)$_3$ moiety such as Gd(hfa)$_3$·L (where L = 2-*R*-4,4,5,5-tetramethyl-4,5-dihydro-1*H*-imidazolyl-1-oxyl-3-oxide; *R* = isopropyl, ethyl, phenyl).[25] This is consistent with the higher coordination number of the gadolinium ion in adduct **2**. The structural data of **2** may be also compared to the data of the fluorine-free monomeric Gd(tmhd)$_3$·monoglyme adduct.[26] The mean value (2.394 Å) of the Gd−O_{hfa} distances of **2** is slightly longer than the average value (2.333 Å) of the Gd−O_{tmhd} distances in the eight-coordinated Gd(tmhd)$_3$·monoglyme. In contrast, the mean value of the Gd−$O_{diglyme}$ bond lengths (2.544 Å) is shorter than the average (2.575 Å) Gd−$O_{monoglyme}$ distances. This is indicative of stronger M−O_{glyme} bonds in the present Gd(hfa)$_3$·diglyme than in the Gd(tmhd)$_3$·monoglyme adduct as a consequence of the electron-withdrawing effect of the CF_3 groups. In fact the electron-withdrawing effect due to the fluorinated groups may render the metal ion more susceptible to nucleophilic attack and favor the formation of strong coordinative bonds between the metal center and the atoms of the diglyme.[19a]

Finally, the structure of Gd(hfa)$_3$·diglyme resembles that of the lanthanum La(hfa)$_3$·diglyme[21] analogue. In the gadolinium compound, however, a large difference (0.150 Å) is observed between the mean Gd−$O_{diglyme}$ and the mean Gd−O_{hfa} distances, while in the lanthanum congener, comparable values have been observed for the mean La−$O_{diglyme}$ and the mean La−O_{hfa} bond lengths, 2.547 and 2.533 Å, respectively. This observation may be likely related to the smaller ionic radius of the gadolinium(III) vs that of the lanthanum(III) ion.

MOCVD Depositions. GdF_3 films have been grown on glass and (111) Si single-crystal substrates. The crystallinity of the film increases upon increasing the deposition temperature and the oxygen flow. The X-ray diffraction pattern of a GdF_3 film obtained at 530 °C is reported in Figure 4. Different preferential orientations of the crystallites have been observed depending on the temperature. Further investigations are in progress and will be reported elsewhere. Wavelength-dispersive X-ray (WDX) analyses are indicative of minor (<3%) amounts of carbon or oxygen contaminations. Note that using the present adducts the fluorinating agent is supplied from the source material itself.

Discussion

The "first-generation" gadolinium *β*-diketonates (e.g., [Gd(tmhd)$_3$]$_2$, Gd(acac)$_3$·*x*H$_2$O, "Gd(hfa)$_3$") are unlikely to represent suitable molecular precursors for MOCVD applications since their extensive use has been hampered either by the low volatility and/or thermal instability[13b,27] due to the pronounced tendency of the central lanthanide ion to expand the coordination number by oligomerization and/or coordination of ancillary solvent molecules.[1] In this context, it must be remembered that the best MOCVD performances have been found, as far as the closely related alkaline-earth-metal precursors are concerned, by using a combination of fluorinated *β*-diketone and polyether ligands.[15−20] By contrast, the fluorine-free *β*-diketone ligands (such as Htmhd) form 1:1 unstable adducts that decompose upon sublimation.[16,17] Analogous properties have been found for the La(tmhd)$_3$·tetraglyme.[28] Recently, Baxter et al.[26] have reported on effects of polyether ligands on the stabilities of "Gd(tmhd)$_3$" complexes and found that the monomeric species with monoglyme and diglyme, such as Gd(tmhd)$_3$·polyether, decompose upon sublimation.[26] Longer polyethers such as the tri-, tetra-, and heptaglyme form dimeric [Gd(tmhd)$_3$]$_2$·polyether adducts that sublime intact.[26]

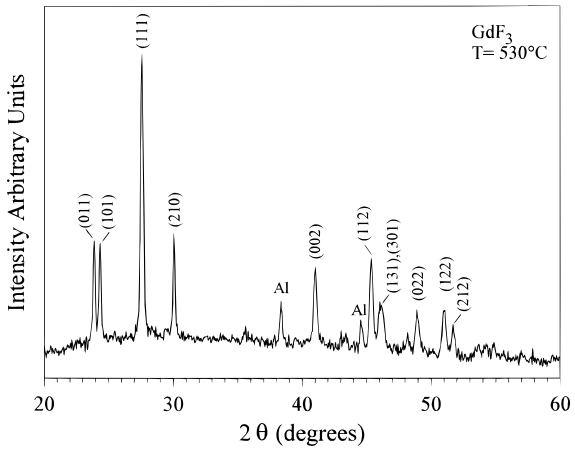

Figure 4. X-ray diffraction pattern of an MOCVD grown GdF_3 film on a (111) Si substrate using the Gd(hfa)$_3$·diglyme as single-source precursor.

In this perspective, novel more suitable molecular architectures for gadolinium sources with improved thermal stabilities and volatilities have been based on a combination of fluorinated *β*-diketones and polyethers to build reproducibly monomeric adducts with suitable properties for MOCVD application. As a matter of fact, the coordination of monoglyme and diglyme to "Gd(hfa)$_3$" results in the formation of thermally stable, volatile, monomeric, water-free Gd(hfa)$_3$·polyether 1:1 adducts (**1** and **2**) which have been successfully applied to MOCVD of GdF_3 films. Films have been deposited from the liquid phase (100−110 °C source temperature). This represents an important issue for MOCVD application,[10] where liquid source precursors are the most desirable due to the greater stability of the vapor pressure and to the absence of any effects of crystallite sizes on the precursor evaporation rate and, hence, on the film growth rate.[29] Note that the crystallite sizes may be responsible for changes of evaporation rates in different

(25) (a) Benelli, C.; Caneschi, A.; Gatteschi, D.; Laugier, J.; Rey, P. *Angew. Chem., Int. Ed. Engl.* **1987**, *26*, 913. (b) Benelli, C.; Caneschi, A.; Gatteschi, D.; Pardi, L.; Rey, P. *Inorg. Chem.* **1989**, *28*, 275. (c) Benelli, C.; Caneschi, A.; Gatteschi, D.; Pardi, L.; Rey, P. *Inorg. Chem.* **1990**, *29*, 4223.

(26) Baxter, I.; Drake, S. R.; Hursthouse, M. B.; Abdul Malik, K. M.; McAleese, J.; Otway, D. J.; Plakatouras, J. C. *Inorg. Chem.* **1995**, *34*, 1384.

(27) Richardson, M. F.; Wagner, W. F.; Sands, D. E. *Inorg. Chem.* **1968**, *7*, 2495.

(28) Drake, S. R.; Lyons, A.; Otway, D. J.; Slawin, A. M. Z.; Williams, D. J. *J. Chem. Soc., Dalton Trans.* **1993**, 2379.

(29) Hitchman, M. L.; Shamlian, S. H.; Gilliland, D. C.; Cole-Hamilton, D.; Nash, J. A. P.; Thompson, S. C.; Cook, S. L. *J. Mater. Chem.* **1995**, *5*, 47.

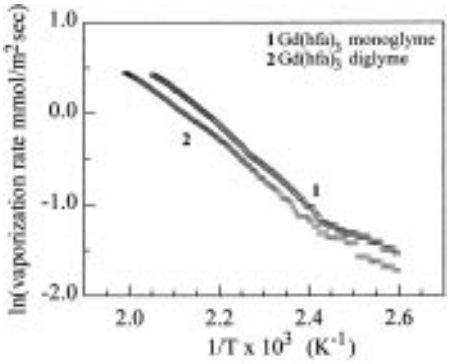

Figure 5. Atmospheric-pressure vaporization rates of the Gd(hfa)$_3$·monoglyme and Gd(hfa)$_3$·diglyme adducts in function of temperature.

experiments and, even more important, of variations during the same experiment.[29]

The "thermal robustness" and mass-transport properties of **1** and **2** have been investigated on samples heated at 110 °C for 3 h in air and left on "open benches" for seven days. Identical TG data have been observed for both the fresh and the "treated" samples. This behavior can be contrasted with the TG data of the Gd(hfa)$_3$·2H$_2$O after the same treatment. In this case, there is evidence that the "treated" sample provides a lower vapor pressure than the fresh material.[30] In addition, the present adducts show a linear dependence of the atmospheric pressure TG volatilization rates upon the temperature (Figure 5) thus indicating greater thermal stability compared with the parent Gd(hfa)$_3$·2H$_2$O, whose sublimation occurs in different steps with decomposition (Figure 1).

Thermal data of **1** and **2** are compared with data of some gadolinium complexes in Table 4. Sublimation temperatures of both adducts represent the lowest values so far reported for gadolinium complexes.

Finally, note that our synthetic strategy produces nonhygroscopic adducts with very high yields (≈90%) in a single-step, low-cost route from commercially available chemicals. This is an important issue for materials used for CVD applications where low-cost chemicals that may be manipulated on open benches are an important objective.[10]

(30) Note that the treated Gd(hfa)$_3$·2H$_2$O sample leaves a much greater residue (32%) at 430 °C than the fresh material.

Table 4. Thermal Data of β-Diketone-Based Gd Precursors

complex	sublimation temp (°C)[a]	melting point (°C)	ref
Gd(hfa)$_3$·monoglyme	75−80	80−81	this work
Gd(hfa)$_3$·diglyme	75−85	see DSC section	this work
Gd(hfa)$_3$·2H$_2$O	decomposes on sublimation	110−121	this work, 13b
[Gd(tmhd)$_3$]$_2$	110−148	176−177	28
Gd(tmhd)$_3$·monoglyme	decomposes on sublimation	117−130	28
Gd(tmhd)$_3$·diglyme	decomposes on sublimation	77−78	28
[Gd(tmhd)$_3$]$_2$·triglyme	110−135	119−121	28
[Gd(tmhd)$_3$]$_2$·tetraglyme	85−165	89−91	28
[Gd(tmhd)$_3$]$_2$·heptaglyme	75−130	82−84	28

[a] The sublimation temperatures are referred to experiments carried out at 10^{-3} mmHg.

Conclusions

The coordination of monoglyme and diglyme to the "Gd(hfa)$_3$" yielded monomeric, nonhygroscopic, low-melting point, volatile, and thermally stable adducts **1** and **2**. The thermal and mass-transport properties have been investigated by atmospheric pressure vaporization rate TG experiments, DSC, and depositions of GdF_3 films. It has been found that the present adducts have better mass-transport properties and thermal behaviors than conventional rare-earth MOCVD precursors and may be successfully applied to GdF_3 film depositions. To our knowledge, they represent the first examples of gadolinium precursors that can be used in the liquid phase without decomposition, thus providing constant evaporation rates even for very long deposition times. These properties, together with the easy one-pot synthetic strategy, render **1** and **2** very attractive MOCVD precursors.

Acknowledgment. The authors thank the Consiglio Nazionale delle Ricerche (CNR, Rome, Progetto Nazionale Materiali Avanzati) for financial support.

Supporting Information Available: Complete lists of bond lengths and angles as well as of anisotropic displacement parameters (4 pages); listing of observed and calculated structure factors (15 pages). Ordering information is given on any current masthead page.

CM950569C